

A simple analytical model of laser direct-drive thin shell target implosion

Bo Yu(余波), Tianxuan Huang(黄天晅), Li Yao(姚立), Chuankui Sun(孙传奎), Wanli Shang(尚万里),Peng Wang(王鹏), Xiaoshi Peng(彭晓世), Qi Tang(唐琦), Zifeng Song(宋仔峰), Wei Jiang(蒋炜),Zhongjing Chen(陈忠靖), Yudong Pu(蒲昱东), Ji Yan(晏骥), Yunsong Dong(董云松),Jiamin Yang(杨家敏), Yongkun Ding(丁永坤), and Jian Zheng(郑坚)

Citation: Chin. Phys. B, 2022, 31 (**4**): 045204. DOI: 10.1088/1674-1056/ac21bd
Journal homepage: http://cpb.iphy.ac.cn; http://iopscience.iop.org/cpb

What follows is a list of articles you may be interested in

First polar direct-drive exploding-pusher target experiments on the ShenGuang laser facility

Bo Yu(余波), Jiamin Yang(杨家敏), Tianxuan Huang(黄天晅), Peng Wang(王鹏), Wanli Shang(尚万里), Xiumei Qiao(乔秀梅), Xuewei Deng(邓学伟), Zhanwen Zhang(张占文), Zifeng Song(宋仔峰), Qi Tang(唐琦), Xiaoshi Peng(彭晓世), Jiabin Chen(陈家斌), Yulong Li(理玉龙), Wei Jiang(蒋炜), Yudong Pu(蒲昱东), Ji Yan(晏骥), Zhongjing Chen(陈忠靖), Yunsong Dong(董云松), Wudi Zheng(郑无敌), Feng Wang(王峰), Shaoen Jiang(江少恩), Yongkun Ding(丁永坤), Jian Zheng(郑坚)

Chin. Phys. B, 2019, 28 (**9**): 095203. DOI: 10.1088/1674-1056/ab37f4

Influence analysis of symmetry on capsule in six-cylinder-port hohlraum

You Zou(邹游), Wudi Zheng(郑无敌), Xin Li(李欣)

Chin. Phys. B, 2019, 28 (**3**): 035203. DOI: 10.1088/1674-1056/28/3/035203

Numerical simulation of the multiple reversed shear Alfvén eigenmodes associated with the triangularity Alfvén gap

Wenjia Wang(王文家), Deng Zhou(周登), Youjun Hu(胡友俊), Yue Ming(明玥), Baolong Hao(郝保龙)

Chin. Phys. B, 2018, 27 (**12**): 125202. DOI: 10.1088/1674-1056/27/12/125202

Conversion of an atomic to a molecular argon ion and low pressure argon relaxation

M N Stankov, A P Jovanović, V Lj Marković, S N Stamenković

Chin. Phys. B, 2016, 25 (**1**): 015204. DOI: 10.1088/1674-1056/25/1/015204

Diagnostic technique for measuring fusion reaction rate for inertial confinement fusion experiments at Shen Guang-III prototype laser facility

Wang Feng, Peng Xiao-Shi, Kang Dong-Guo, Liu Shen-Ye, Xu Tao

Chin. Phys. B, 2013, 22 (**11**): 115204. DOI: 10.1088/1674-1056/22/11/115204

A simple analytical model of laser direct-drive thin shell target implosion

Bo Yu(余波)[1,2,†], Tianxuan Huang(黄天晅)[2], Li Yao(姚立)[2], Chuankui Sun(孙传奎)[2], Wanli Shang(尚万里)[2], Peng Wang(王鹏)[2], Xiaoshi Peng(彭晓世)[2], Qi Tang(唐琦)[2], Zifeng Song(宋仔峰)[2], Wei Jiang(蒋炜)[2], Zhongjing Chen(陈忠靖)[2], Yudong Pu(蒲昱东)[2], Ji Yan(晏骥)[2], Yunsong Dong(董云松)[2], Jiamin Yang(杨家敏)[2], Yongkun Ding(丁永坤)[1,3], and Jian Zheng(郑坚)[1,4]

[1] *School of Nuclear Science and Technology, University of Science and Technology of China, Hefei* 230026, *China*
[2] *Research Center of Laser Fusion, China Academy of Engineering Physics, Mianyang* 621900, *China*
[3] *Institute of Applied Physics and Computational Mathematics, Beijing* 100088, *China*
[4] *IFSA Collaborative Innovation Center, Shanghai Jiao Tong University, Shanghai* 200240, *China*

(Received 3 July 2021; revised manuscript received 11 August 2021; accepted manuscript online 27 August 2021)

A high-neutron yield platform imploded by a thin shell target is generally built to probe nuclear science problems, and it has the advantages of high neutron yield, ultrashort fusion time, micro fusion zone, isotropic and monoenergetic neutron. Some analytical models have been proposed to interpret exploding-pusher target implosion driven by a long wavelength laser, whereas they are imperfect for a 0.35 μm laser implosion experiment. When using the 0.35 μm laser, the shell is ablated and accelerated to high implosion velocity governed by Newton's law, ablation acceleration and quasi-adiabatic compression models are suitable to explain the implosion of a laser direct-drive thin shell target. The new analytical model scales bang time, ion temperature and neutron yield for large variations in laser power, target radius, shell thickness, and fuel pressure. The predicted results of the analytical model are in agreement with experimental data on the Shenguang-III prototype laser facility, 100 kJ laser facility, Omega, and NIF, it demonstrates that the analytical model benefits the understanding of experiment performance and optimizing the target design of high neutron yield implosion.

Keywords: direct drive, analytical model, thin shell target, neutron yield

PACS: 52.57.–z, 52.38.Mf, 24.10.Nz, 29.25.Dz **DOI:** 10.1088/1674-1056/ac21bd

1. Introduction

The thin shell target implosion experiment of the laser direct drive is designed to develop a high-neutron yield platform. The implosion is that the high-intensity laser directly interacts with a thin shell, such as a plastic or glass wall, to generate a strong shock wave, heat and compress the fuel, and produce thermonuclear neutrons when the strong shocks collide at the target center. Such a platform has the advantages of high neutron yield, ultrashort fusion time, micro fusion zone, isotropic and monoenergetic neutron, and is usually used to develop the nuclear diagnostic system,[1,2] study the neutron irradiation effect,[3] measure the nuclear reaction[4,5] and cross section,[6] probe the fluid kinetic effects,[7–10] *et al.* The glass target implosion is the simplest and earliest experiment on the laser facility, and demonstrates that thermonuclear neutrons resulting from laser-induced microshell implosion at KMS.[11]

In order to understand the functional relationships between the various parameters of experiments and increase experiential neutron yield, some analytical models for long wavelength laser, such as 1.05 μm, have been proposed. Storm *et al.*[12] developed a simple model of glass target with high fill gas density to scale neutron yield for variations in laser power, pulse length, target radius, wall thickness and fuel pressure, and the deviation of neutron yield within a factor of 2 for laser wavelength of 1.06 μm. The model of Giovannielli *et al.*[13] was similar to Storm's, but the effect of shell density was considered. Rosen *et al.*[14] assumed that the ion was heated by a shock followed by isentropic compression, and the compression was calculated by the conservation of mass and density profile assumption. The neutron yield predicted by the Rosen model agreed over a broad range of parameter space, and the experimental yield on the Janus, Argus, and Shiva scaled roughly as the absorbed laser power squared. Based on the Rosen model, Ahlborn *et al.*[15] carried the initial compression further to include reflected shocks. The improved model was more useful than other model in describing density, area density, and ion temperature with the variation of fill gas pressure. Andreev *et al.*[16] provided a unified description of heating and compression regimes, the model predicted results and the experimental data on neutron yield was better than within two orders of magnitude. Kitagawa *et al.*[17] optimized the target for the maximum number of neutrons at a given energy on the Gekko MII two-beam 1.05 μm laser system, showed neutron yield is proportional to the laser power of 2.4 power. Zhang *et al.*[18] analyzed a large number of experiment data and developed a simple theoretical model for the 1.05 μm laser to calculate compression ratio, ion temperature, confinement time and neutron yield. neutron yield agreed with

[†]Corresponding author. E-mail: yubobnu@163.com

© 2022 Chinese Physical Society and IOP Publishing Ltd

the experimental results within a factor of 2 to 3.

These existing analytical models[12–18] have been properly used to interpret thin shell glass target implosion with a long wavelength laser ($\lambda \geq 0.53$ μm). While the high intensity, long wavelength laser interacts with glass, resonance absorption is important[19] and the electrons are preferentially heated. The electron thermal wave rapidly propagates through glass and into the fuel at near supersonic speeds. Because of the high density of glass, the electron–ion equilibrium time is short ($\sim$ 1 ps) , ion temperature rises quickly, and glass shell is integrality heated to a pressure of several million pascals. Under this high pressure, the shell explodes. Roughly half of glass wall explodes outward, the remaining wall moves inward. The inward wall acts as a piston, driving a shock heat the ion. Behind the shock, the glass shell also moves inward, isentropically compresses the post-shock fuel gas, and further heats the ions to thermonuclear fusion temperature. Finally, fuel gas is heated to several keV to tens of keV by shock and isentropic compression, fusion reaction occurs and produces a large number of thermonuclear neutrons until the fuel cools and disassembles.

When using the 0.35 μm laser to drive glass target imploding, the dominant energy absorption mechanism is inverse bremsstrahlung,[19] energy depositing process is obviously different from that of long wavelength laser. The shell is ablated and accelerated to high implosion velocity governed by Newton's law, these existing analytical models are imperfect for the thin shell target implosion driven by 0.35 μm laser.

This article proposes a new analytical model to describe thin shell target implosion with a 0.35 μm laser, including ablation acceleration and quasi-adiabatic compression process. The bang time, ion temperature and neutron yield predicted by the analytical model are compared with the experimental results.

2. Analytical model

Figure 1 shows the density evolution diagram of thin shell target implosion driven by a 0.35 μm laser, and is simulated by Multi1D.[20] The surface layer of the target shell is irradiated by the 0.35 μm laser, and the laser energy is deposited at the critical surface and propagated by electron heat conduction. With the same laser intensity, the electron temperature is much lower than that generated by long wavelength laser, only the outer layer is ablated and ionized, and then expands outward. The recoil of ablating and expanding material is the ablation pressure. As the ablator expands outward, momentum conservation forces the rest of shell to accelerate the inward flight under the action of ablation pressure, and a shock wave propagates through the shell and into the fuel. The shock heats and compresses the fuel and reflects at the target center. The reflected shock collides with the inward flying shell, which makes the shell decelerate and the reflected shock rebounds again. When the gas pressure is close to the pressure of the shell, the shell starts to be decelerated until the implosion velocity drops to zero. Then hot-spot pressure and ion temperature reach its maximum, and fusion reaction also arrives at the peak. It can be seen that the existing models are not suitable for short pulse laser experiments, and ablation acceleration and quasiadiabatic compression models are needed to explain the physical process of thin shell target implosion.

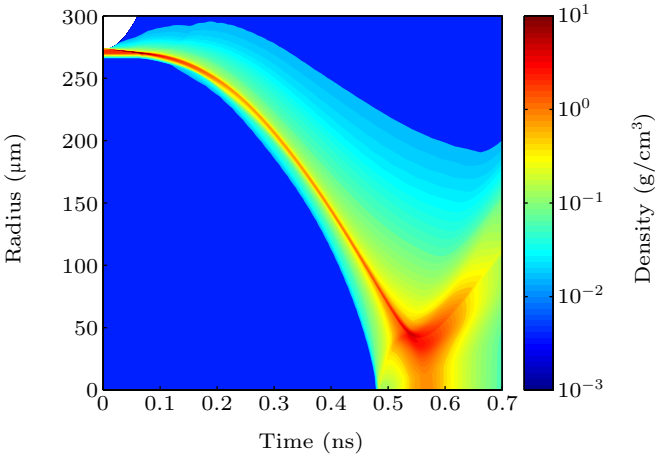


Fig. 1. The density evolution of thin shell target implosion.

For laser direct drive thin shell target implosion, the ablation pressure is relative to the intensity I_{15} (in 10^{15} W/cm^2) and wavelength λ (in μm) of incident laser, approximately,[21]

$$p_{\rm a} = 40\,(I_{15}/\lambda)^{2/3}. \tag{1}$$

The capsule shell is only several microns in thickness and quickly accelerates to high velocity. The implosion bang time is very short and deceleration process can be nearly ignored, so the shell velocity scales with target initial radius R and acceleration time $t_{\rm accl}$ is $u_{\rm imp} = 2R_0/t_{\rm accel}$. Based on Newton's law $M_{\rm shell}u_{\rm imp}/t_{\rm accel} = 4\pi R_0^2 P_{\rm a}$, the shell velocity

$$u_{\rm imp}^2 = \frac{8\pi R_0^3 P_{\rm a}}{M_{\rm shell}}. \tag{2}$$

Using Eq. (2) with the shell mass $M_{\rm shell} = \rho_{\rm s} 4\pi R_0^2 \Delta R$, where $\rho_{\rm s}$ is the shell density and ΔR is the shell thickness, the shell velocity scales as

$$u_{\rm imp} = \sqrt{\frac{2R_0 P_{\rm a}}{\rho_{\rm s}\Delta R}} \sim \sqrt{\frac{R_0 I_{15}^{2/3}}{\Delta R}}. \tag{3}$$

And the implosion bang time of thin shell target is

$$t = \frac{2R_0}{u_{\rm imp}} \sim \frac{R_0^{1/2}\Delta R^{1/2}}{I_{15}^{1/3}}. \tag{4}$$

Equation (4) indicates that the implosion bang time is dependent on the target radius and shell thickness, and the laser intensity.

From the strong shock relation

$$\begin{aligned} u_{\rm D}-u_0 &= \frac{2}{\gamma+1}(D-u_0),\\ \rho_{\rm D} &= \frac{\gamma+1}{\gamma-1}\rho_0,\\ p_{\rm D} &= \frac{2}{\gamma+1}\rho_0(D-u_0)^2, \end{aligned} \tag{5}$$

where D is the strong shock velocity, u_0 and $u_{\rm D}$ are the velocity of shock and post-shock, ρ_0 and $\rho_{\rm D}$ are the density of shock and post-shock, and $p_{\rm D}$ is the pressure of post-shock.

The initial fluid is static ($u_0 = 0$). By assuming the velocity at the fluid interface is continuous, post-shock velocity is equal with the shell velocity, post-shock pressure

$$p_{\rm D} = \frac{\gamma-1}{2}\rho_{\rm D}(u_{\rm D}-u_0)^2 = \frac{\gamma-1}{2}\rho_{\rm D}u_{\rm imp}^2. \tag{6}$$

Then the shock propagates inwards, rebounds at the target center, and reflects again when colliding with the shell. Accordingly, the fusion fuel is serially compressed by the first shock, the reflected shock, and the final quasi-adiabatic process, and reaches the maximum fuel density[15] $\rho = 2.19\rho_{\rm s}^{1/\gamma}\rho_0^{1-1/\gamma}$ and the minimum radius[15] $R = 0.66R_0\rho_0^{1/3\gamma}$. From the adiabatic compression $(p/p_0) = (\rho/\rho_0)^\gamma$, the pressure of the compressed fuel gas can be written as

$$p = p_0\left(\frac{\rho}{\rho_0}\right)^\gamma = \frac{\gamma-1}{2}\rho_0 u_{\rm imp}^2\left(\frac{\rho}{\rho_0}\right)^\gamma. \tag{7}$$

In general, the ion is heated by the shock and adiabatic compression, and the internal energy of the fuel is equal to kinetic energy. According to the equation of state of the ideal gas $p = \rho\Re T_{\rm i}/\mu$, where μ is molar mass, $\Re$ is universal constant. The ion temperature at implosion bang time is as follows:

$$T_{\rm i} = \frac{\mu}{\rho\Re}p = \frac{\gamma-1}{2}\frac{\mu}{\Re}\left(\frac{\rho}{\rho_0}\right)^{\gamma-1}u_{\rm imp}^2. \tag{8}$$

Then, using Eq. (3) and maximum fuel density,

$$T_{\rm i} \sim \frac{u_{\rm imp}^2}{\rho_0^{(\gamma-1)/\gamma}} \sim \frac{R_0 I_{15}^{2/3}}{\Delta R\rho_0^{2/5}}. \tag{9}$$

Equation (4) shows that the ion temperature increases by reducing shell thickness and fuel initial density or increasing the target radius at a given laser intensity.

Neglecting fuel depletion, the neutron yield for DT plasma is defined as

$$Y_{\rm n} = \int {\rm d}t\int {\rm d}^3 r N_{\rm D}N_{\rm T}\langle\sigma v\rangle_{\rm DT}, \tag{10}$$

where $\langle\sigma v\rangle_{\rm DT}$ is the cross section of DT reaction and proportional to the square of ion temperature in several keV. $\int {\rm d}^3 r N_{\rm D}N_{\rm T}$ is the fuel mass and equal to the initial fuel mass $\rho_0\times 4\pi R_0^3/3$ according to the conservation of mass. $\int {\rm d}t$ is the confinement time of the thermonuclear reaction of DT plasma. The confinement time is defined as the time interval between the rarefaction wave traverses to radius R of the burning core. Since the arrival times of the rarefaction wave at different points in space is different, the confinement time is calculated by the spatial average

$$\overline{\Delta t} = \frac{\int_0^R \frac{R-r}{c_{\rm S}}r^2{\rm d}r}{\int_0^{R_0} r^2{\rm d}r} = \frac{R}{4c_{\rm S}} \sim \frac{R_0\rho_0^{1/5}}{4}\left(\frac{\mu}{\gamma\Re T_{\rm i}}\right)^{1/2}. \tag{11}$$

Combining Eqs. (9) and (11), equation (10) can be written in the form

$$\begin{aligned} Y_{\rm n} &= \frac{1}{2}\int {\rm d}t\int {\rm d}^3 r N_{\rm D}^2\langle\sigma v\rangle_{\rm DD} \sim \frac{R_0\rho_0^{1/5}}{\sqrt{T_{\rm i}}}\times R_0^3\rho_0\times T_{\rm i}^2\\ &= R_0^4\rho_0^{6/5}T_{\rm i}^{1.5} \sim \frac{\rho_0^{0.6}I_{15}R_0^{5.5}}{\Delta R^{1.5}}. \end{aligned} \tag{12}$$

According to Eq. (12), the lower initial gas density, the bigger initial radius and the thinner shell thickness benefits the higher neutron yield.

3. Comparing with experiment

In order to validate the analytical model of thin shell target implosion, the DD and DT experimental data at Shenguang-III prototype laser facility, 100 kJ laser facility, Omega and NIF are compared with the analytical model. The target diameters on the Shenguang-III prototype laser facility and 100 kJ laser facility[22] were ~ 540 μm and ~ 720 μm, the glass wall thickness were ~ 2.6 μm and ~ 2 μm, the plastic wall thickness were ~ 1 μm, and the DT or DD gas was 10–45 atm. The capsule diameters were ~ 1100 μm used on the Omega[23] and ~ 1500 μm used on the NIF,[24–26] the glass wall was more thicker and the same with ~ 4.5 μm, and the DT or DD gas was 5–10 atm.

The implosion bang time was measured by the neutron fusion reaction rate diagnostic system[27] on the 100 kJ laser facility, and less than 700 ps.[22] The measurement error was more than 200 ps in 2015 and decreases to 50 ps after 2018. The Omega bang time was diagnosed by neutrons and gammas, and more than 1.4 ns.[23] The NIF bang time was got by neutrons or x-ray, and much more later[24–26] because of the larger target. The comparison of bang time between experimental results and predicted results is show in Fig. 2. The experimental results of 100 kJ laser facility and NIF are consistent with the predicted results of the analytical model, but the experimental results of Omega deviate from the predicted results. The potential reason of the discrepancy between experiment and model is the laser absorption efficiency. The 60-beam Omega laser is arranged in "stretched soccer-ball" configuration,[28] the incident angle of laser is smaller than the

100 kJ laser facility and NIF, and laser absorption efficiency and implosion efficiency is higher, resulting in the shorter implosion time and the higher yield-over-clean.

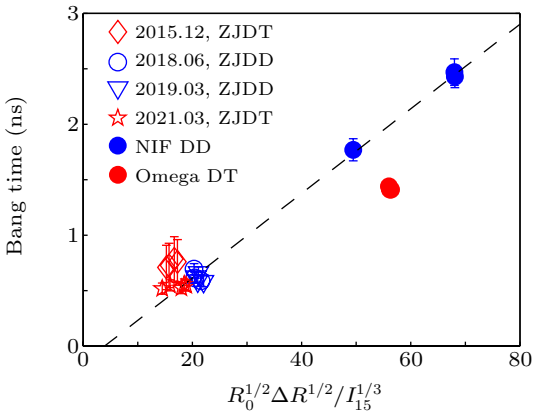


Fig. 2. Comparison of bang time between experiment and model.

Figure 3 shows the comparison of ion temperature between experimental results and analytical model. The ion temperature was deduced from the nToF spectrum[29] on the 100 kJ laser facility, Omega and NIF. In Fig. 3, the measured results of ion temperature is proportional to the predicted results of the analytical model except two shots. One of them is the first experimental result with high ion temperature on the 100kJ laser facility. The nToF detector was first used to measure the high ion temperature, the signal is close to saturation, and measurement result is larger than the other shots. Another experimental result is shot N120328 on the NIF, which is imploded with the greatest laser power,[24] causing the burn averaged ion temperature and neutron yield is higher, bang time is shorter than the other shots.

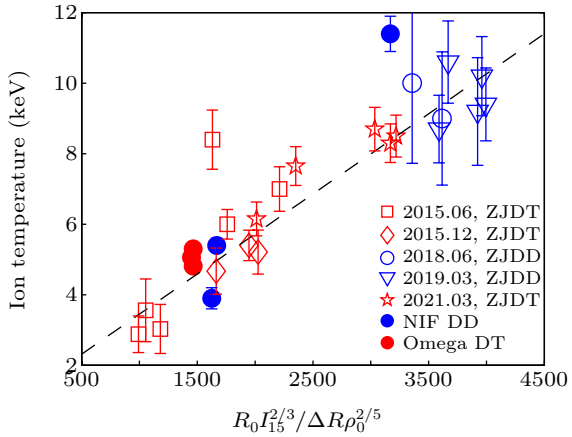


Fig. 3. Comparison of ion temperature between experiment and model.

On the Shenguang-III prototype and 100 kJ laser facility, the DD neutron yield was measured by plastic detector[30] before 2014 and indium activation system[31] after 2014, the DT neutron yield was measured by copper activation system.[32] The Omega and NIF neutron yields were diagnosed by the nTOF detector.[23,24] In the year of 2014, glass targets were imploded by 32 beam laser on the 100 kJ laser facility. In order to compare between the experiment and model, DT neutron yield was converted to DD neutron yield, and the effect of the ion number density and gas pressure were corrected. The comparison of neutron yield is shown in Fig. 4. Except for the experiment data in 2015 and on the Omega, the experimental results are in good agreement with the analytical model in three orders of magnitude. The neutron yield of the Φ540 μm capsule on the 100 kJ laser facility in 2015 and the neutron yield on the Omega is slightly higher than the predicted results. One of reason is that the laser absorption efficiency is higher. The repointing distance of the Φ540 μm target is very short, the laser incident angle is small, then the laser absorption efficiency is higher, which is the same as the Omega. Another reason is that the laser irradiation uniformity is better. For the Φ540 μm target on the 100 kJ laser facility, the final irradiation uniformity is less than 4%.[22] The irradiation uniformity on the Omega is better than 1%[28] because of the laser arrange of the direct drive.

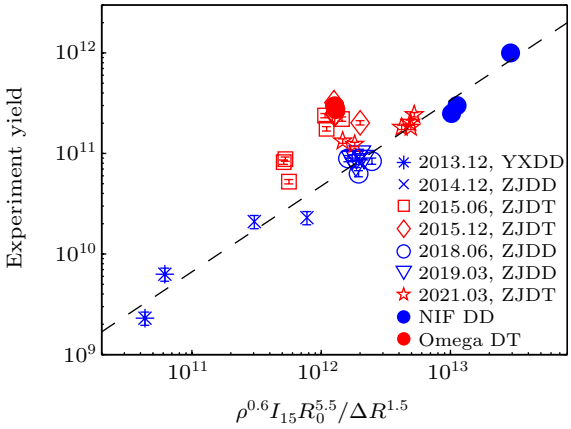


Fig. 4. Comparison of neutron yield between the experiment and model.

The experimental results in Figs. 2–4 are in good agreement with the analytical results, indicating that the ablation acceleration and quasi-adiabatic compression models can be used to properly describe the implosion physical process of the thin shell target driven by the short wavelength laser, and can be used for the optimization design of a high neutron yield experiment.

4. Conclusion

A simple analytical model of laser direct-drive thin shell target implosion for 0.35 μm laser is developed. When the 0.35 μm laser is used to drive thin shell target imploding, the laser energy absorption mechanism is different from that of the long wavelength laser. The dominant mechanism is inverse bremsstrahlung, the shell is ablated and accelerated to high implosion velocity governed by Newton's law, and ablation acceleration and quasiadiabatic compression models are suitable to explain the physical process of laser direct-drive thin

shell target implosion. The new analytical model scales bang time, ion temperature and neutron yield for large variations in laser power, target radius, shell thickness and fuel pressure. The predicted results of the analytical model are in agreement with experimental results on the Shenguang-III prototype laser facility, 100 kJ laser facility, Omega and NIF, demonstrates that the new analytical model is useful in understanding the functional relationships of the parameters of experiments and optimizing the target design of high-neutron yield implosion.

Acknowledgments

The authors would like to thank the staffs of the Shenguang-III prototype and 100 kJ laser facility for their co-operation. Project supported by the National Natural Science Foundation of China (Grant Nos. 11775203 and 12075219) and the Innovation and Development Fund of China Academy of Engineering Physics (Grant No. CX20210019).

References

[1] Rinderknecht H G, Johnson M G, Zylstra A B, *et al.* 2012 *Rev. Sci. Instrum.* **83** 10D902
[2] Waugh C J, Rosenberg M J, Zylstra A B, *et al.* 2015 *Rev. Sci. Instrum.* **86** 053506
[3] Dayton M, Datte P, Carpenter A, *et al.* 2017 *Proc. SPIE* **10390** 1039007
[4] Casey D T, Sayre D B, Brune C R, *et al.* 2017 *Nat. Phys.* **13** 1227
[5] Zylstra A B, Frenje J A, Johnson M G, *et al.* 2017 *Phys. Rev. Lett.* **119** 222701
[6] Frenje J A, Li C K, Seguin F H, *et al.* 2011 *Phys. Rev. Lett.* **107** 122502
[7] Rinderknecht H G, Rosenberg M J, Li C K, *et al.* 2015 *Phys. Rev. Lett.* **114** 025001
[8] Kagan G, Svyatskiy D, Rinderknecht H G, *et al.* 2015 *Phys. Rev. Lett.* **115** 105002
[9] Forrest C J, Radha P B, Knauer J P, *et al.* 2017 *Phys. Rev. Lett.* **118** 095002
[10] Shan L Q, Cai H B, Zhang W S, *et al.* 2018 *Phys. Rev. Lett.* **120** 195001
[11] Campbell P M, Charatis G and Montry G R 1975 *Phys. Rev. Lett.* **34** 74
[12] Storm E K, Ahlstrom H G, Boyle M J, *et al.* 1978 *Phys. Rev. Lett.* **40** 1570
[13] Giovanielli D V and Cranfill C W 1978 *Los Alamos Scientific Lab.* LA-7218-MS
[14] Rosen M D and Nuckolls J H 1979 *Phys. Fluids* **22** 1393
[15] Ahlborn B and Key M H 1981 *Plasma Phys.* **23** 435
[16] Andreev A A and Solovev N A 1985 *Sov. J. Quantum Electron.* **15** 556
[17] Kitagawa Y, Miyanaga N, Kato Y, *et al.* 1986 *Jpn. J. Appl. Phys.* **25** 586
[18] Zhang J, Jiang R H and Zeng X C 1988 *Nuclear Fusion and Plasma Physics* **8** 207 (in Chinese)
[19] Craxton R S, Anderson K S, Boehly T R, *et al.* 2015 *Phys. Plasmas* **22** 110501
[20] Ramis R, Schmalz J and Meyer-ter-Vehn J 1988 *Comput. Phys. Commun.* **49** 475
[21] Lindl J 1995 *Phys. Plasmas* **2** 3933
[22] Yu B, Yang J M, Huang T X, *et al.* 2019 *Chin. Phys. B* **28** 095203
[23] Herrmann H W, Langenbrunner J R and Mack J M 2009 *Phys. Plasmas* **16** 056312
[24] Rosenberg M J, Zylstra A B, Seguin F H, *et al.* 2014 *Phys. Plasmas* **21** 122712
[25] Rinderknecht H G, Rosenberg M J, Zylstra A B, *et al.* 2015 *Phys. Plasmas* **22** 082709
[26] Johnson M G, Zylstra A B, Bacher A, *et al.* 2017 *Phys. Plasmas* **24** 041407
[27] Wang F, Peng X S, Kang D G, *et al.* 2013 *Chin. Phys. B* **22** 115204
[28] Soures J M, McCrory R L, Verdon C P, *et al.* 1996 *Phys. Plasmas* **3** 2108
[29] Chen J B, Zheng Z J, Peng H S, *et al.* 2001 *Rev. Sci. Instrum.* **72** 3534
[30] Chen J B, Feng J, Zheng Z J, *et al.* 1995 *Nuclear Fusion and Plasma Physics* **15** 53 (in Chinese)
[31] Song Z F, Chen J B, Tang Q, *et al.* 2012 *High Power Laser Part. Beams* **24** 1165 (in Chinese)
[32] Song Z F, Tang Q, Chen J B, *et al.* 2015 *High Power Laser Part. Beams* **27** 112005 (in Chinese)